Anisotropic behaviour of etched hardness indentations

At room temperature, normally brittle materials can be made to deform plastically by suppressing brittle failure through the application of a stress system containing a large hydrostatic component. Such a system is prevalent under microhardness indenters. Intrinsic anisotropy in the response of single crystals to Knoop microindentation hardness testing is a well established phenomenon which has been reported for many crystalline solids and has been particularly employed in the study of the plastic deformation modes of brittle materials (e.g. [1, 2]). Dislocation etch-pitting techniques have also often been employed in conjunction with hardness tests to study the dislocation distributions around indentations (e.g. [1, 2]). Such studies have been used to examine slip plane indentities [1–3] and dislocation mobilities (e.g. [3]) but usually only in systems where the slip planes are active to some distance away from the indentation creating familiar etch-pit rosettes. In the harder refractory solids (e.g. SiC [4] and NbC [5]) there is evidence that any plastic deformation, resulting from the indentation process, is highly localized beneath the resultant indentation to the extent that etch rosettes cannot be found. In such a case for SiC, the authors have found that the indentation itself changes shape during etching and that observations of this change can be interpreted to provide otherwise unobtainable information concerning the operating slip planes and the distribution of plastic strain.

The interpretation of the anisotropy of Knoop microhardness values with indenter orientation on single crystal facets is usually based on the "effective resolved shear stress" (ERSS) model of Brookes *et al.* [1, 2]. This hypothesis rests on the premises that the amount of plastic deformation (and thus the apparent hardness) resulting from the indentation is governed by the shear stress distribution in the material under the indenter, the local orientations of the slip systems in this vicinity and the constraints imposed on the operation of these by the rigid indenter geometry itself. Thus Fig. 1 shows an experimental plot of the constant-load Knoop hardness as a function of orientation on the basal $(0\,0\,0\,\bar{1})$ plane of a SiC single crystal. Based on the ERSS model, the best fit to this curve is found assuming that the indentation process on this plane is controlled by a single slip system of the $\{h\,0\,\bar{h}\,l\}\langle 1\,1\,\bar{2}\,0\rangle$ type [6–8]. The model takes no account of either cross-slip or the possible simultaneous operation of different slip modes.

As part of an extensive research programme examining the microhardness behaviour of SiC and

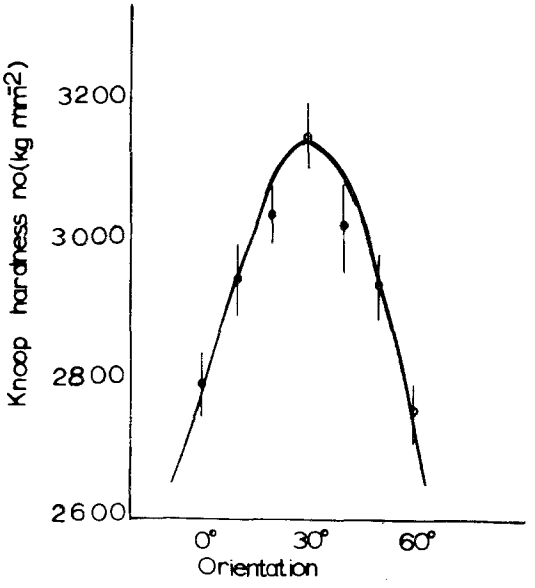

Figure 1 An experimental hardness anistropy curve for a single crystal of SiC indented on the basal $(0\,0\,0\,1)$ plane using a standard Knoop microhardness indenter and a load of 300 g. Orientations of 0° and 60° correspond to the long diagonal of the indenter parallel to $\langle 1\,1\,\bar{2}\,0\rangle$. The harder 30° direction is $\langle 1\,0\,\bar{1}\,0\rangle$.

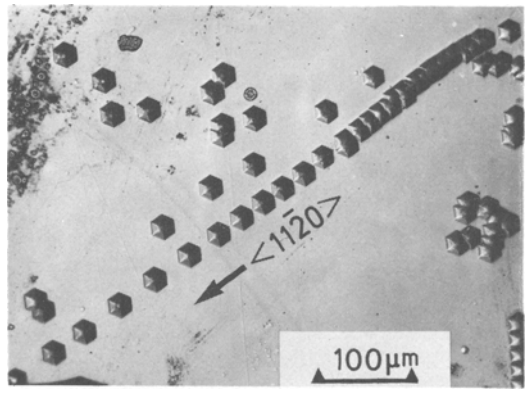

Figure 2 A nominally undeformed SiC single crystal basal plane etched in molten sodium peroxide to reveal dislocation etch pits. The rows of pits are parallel to $\langle 1\,1\,\bar{2}\,0\rangle$ (i.e. the traces of $\{h\,0\,\bar{h}\,l\}$). (Optical micrograph, oblique illumination).

Si_3N_4 materials [6, 9] it was intended to quantitatively reveal dislocation arrangements around microhardness indentations by an etch-pitting technique in order to confirm the ERSS hypothesis. It was initially established that one of the polar (0 0 0 1) faces of as-grown SiC platelet crystals would show well developed dislocation etch pits when etched in molten sodium peroxide at 400° C for approximately 10 min. Such etch pits, resulting from a low "grown in" dislocation density, were almost always well developed regular hexagons bounded by $\langle 1\,1\,\bar{2}\,0\rangle$ directions [4, 9] and examples are shown in Fig. 2. However, because of the highly localized platic flow, attempts to reveal any etch-pits rosettes around indentations were unsuccessful but the indentations themselves were found to change shape during etching. Thus, the etching characteristics of the indentations themselves have been used to reveal information concerning the preferential plastic deformation on certain slip planes.

By taking measurements of the largest and smallest dimensions of these indentations both before and after etching, Table I has been derived for indents specifically parallel to $[1\,1\,\bar{2}\,0]$ and $[1\,\bar{1}\,0\,0]$ respectively. Orthogonal length and width measurements were made parallel to the relevant $\langle 1\,1\,\bar{2}\,0\rangle$ and $\langle 1\,\bar{1}\,0\,0\rangle$ directions on each indentation and these are listed. The aspect ratio $d_{[1\,1\,\bar{2}\,0]}/d_{[1\,\bar{1}\,0\,0]}$ confirms the shape change observed during etching and shows the difference apparent in the behaviour of the indentations of differing orientation. The difference in etching behaviour of two such indents is shown in Fig. 3.

Etching of the material immediately adjacent to an indentation results in two effects. Firstly, material is removed parallel to the original surface so that, in the absence of any further effects, the indentation would be progressively serially-sectioned and, when viewed, would be seen to become progressively smaller in size but with no change in shape. Secondly, preferential etching occurs due to the stored plastic energy distributed around the indentation and this may remove material either parallel or perpendicular to the original surface; that is, the indentation may change its size, overall shape and depth. Thus etching can be regarded as a means of examining the anisotropy of the distribution of stored energy as a function of depth, (although as the indentation depth also changes by etching, this parameter cannot be readily specified even from a sequence of observations at progressively longer etching times).

The important feature of Table I and Fig. 3 is that, after etching, the etched indentation is still found to a have a regular crystallographically specific shape (related to the unetched figure) but that this shape now has a different aspect ratio. By comparing Figs. 3b and d which show the effect of etching, under constant conditions, on Knoop indentations whose long axes were originally parallel to the $[1\,1\,\bar{2}\,0]$ and $[1\,\bar{1}\,0\,0]$ directions respectively, it was observed that for the former, preferential flow had occurred in the specific long direction of the indenter (suggesting that those members of the operating slip system family containing this direction had been predominantly activated), whereas, in the latter case, material around the indentation

TABLE I

Direction of long axis of Knoop indenter	Original Knoop indentation			Etched Knoop indentation		
	$d_{[1\,1\,\bar{2}\,0]}$ (μm)	$d_{[1\,\bar{1}\,0\,0]}$ (μm)	Aspect ratio $\frac{d_{[1\,1\,\bar{2}\,0]}}{d_{[1\,\bar{1}\,0\,0]}}$	$d_{[1\,1\,\bar{2}\,0]}$ (μm)	$d_{[1\,1\,\bar{2}\,0]}$ (μm)	Aspect ratio $\frac{d_{[1\,1\,\bar{2}\,0]}}{d_{[1\,\bar{1}\,0\,0]}}$
(a) $[11\bar{2}0]$	17.20	1.60	10.75	23.33	13.65	1.71
(b) $[1\bar{1}00]$	1.60	15.70	0.10	19.05	19.05	1.00

Changes in aspect ratio of Knoop microhardness indentations as a result of etching to examine the anisotropic distribution of stored plastic energy immediately around and under the indentations. $d_{[1\,1\,\bar{2}\,0]}$ and $d_{[1\,\bar{1}\,0\,0]}$ are the lateral dimensions of the indent in orthogonal directions (these also being the softer and harder Knoop hardness directions respectively). Rows (a) and (b) are equivalent to indents rotated by 30°, but the indexing has been chosen for consistency with the d-values. The "before" and "after"-etching dimensions are not from the same indents on the same crystal, but from nominally identical indents on similar crystals. However, the significant change in the aspect ratio (i.e. morphology) of the indents on etching is unaffected by this. All measurements are from optical micrographs.

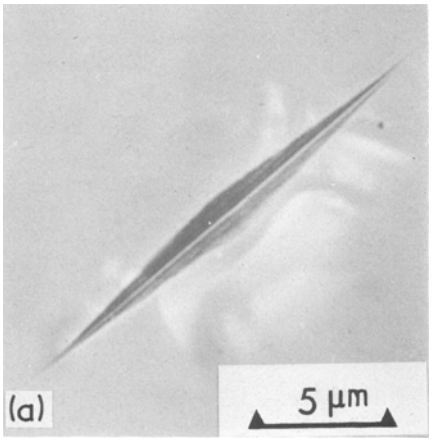

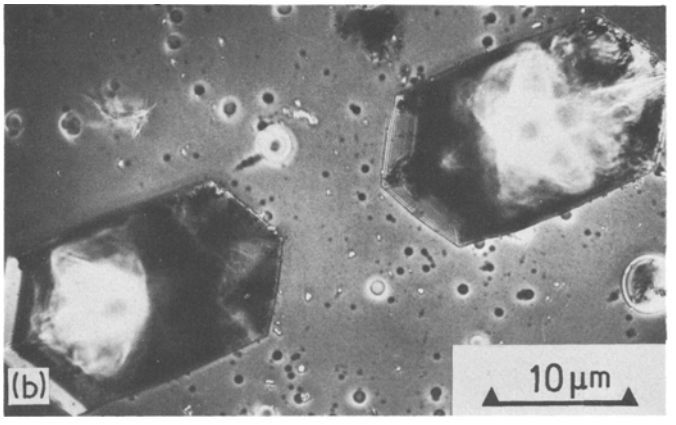

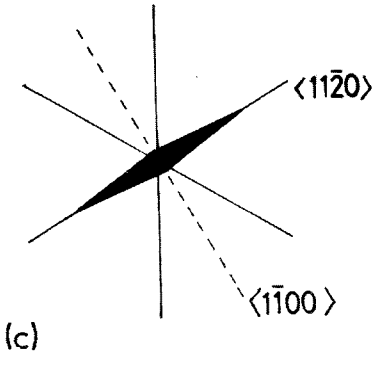

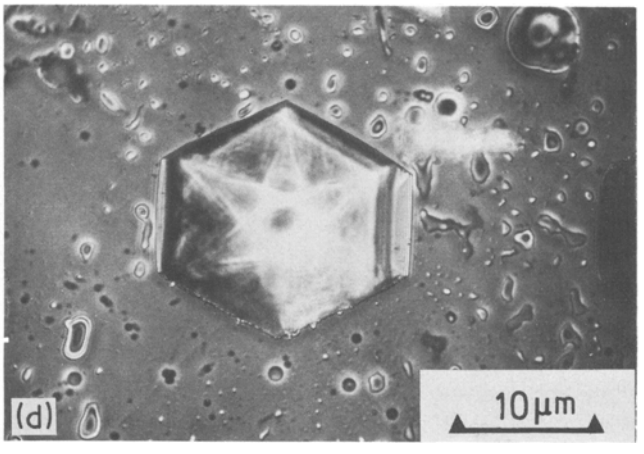

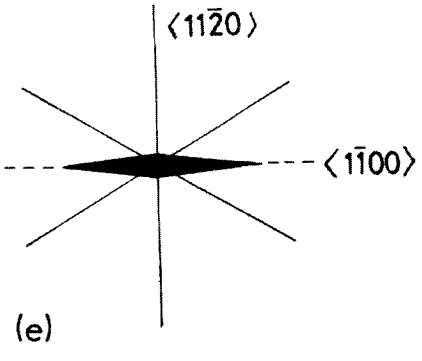

Figure 3 (a) photomicrograph of a [1 1 $\bar{2}$ 0] Knoop indentation (100 g load) showing no cracking and resulting from localized sub-surface plastic flow. (b) Two [1 1 $\bar{2}$ 0] indentations (i.e. softer indentation direction) after etching. (c) Schematic arrangement of the indenter orientation in (b) with respect to the $\{h\,0\,\bar{h}\,l\}$ slip plane traces. (d) and (e) as for (b) and (c) but for a [1 0 $\bar{1}$ 0] indentation (i.e. indenter parallel to the harder indentation direction). (micrographs (b) and (d) were taken using phase contrast techniques.)

had been remoulded in such a way that preferential plastic flow is (approximately) equal in all ⟨1 1 $\bar{2}$ 0⟩ directions (suggesting that, in any given slip plane family, all the $\{h\,0\,\bar{h}\,l\}$ types of slip planes had been activated). In both cases, the change in $d_{[1\,1\,\bar{2}\,0]}/d_{[1\,\bar{1}\,0\,0]}$ (i.e. the aspect ratio) can be consistently interpreted in terms of differing amounts of preferential etching along ⟨1 1 $\bar{2}$ 0⟩, suggesting the maximum stored energy to be located on $\{h\,0\,\bar{h}\,l\}$ planes. From Table I and visual observations of the indentations, the following conclusions may be reached:

(1) the predominantly hexagonal etch pits which are derived from the indentations represent some indication of the extent of plastic deformation within the vicinity of the indentation;

(2) that there is very considerable resultant

plastic flow around the short diagonal of the indenter. This is at variance with the hitherto held view that the geometry of the indenter resulted in predominantly elastic deformation adjacent to the short diagonal [10, 11].

(3) that the $\{h\,0\,\bar{h}\,l\}$ type of slip plane is more active during plastic deformation than the $\{h\,h\,\bar{2}\,\bar{h}\,l\}$ type. This is deduced from the relatively higher rate of growth of the etch pit along the long or short diagonals of the indentation when these coincide with the $\langle 1\,1\,\bar{2}\,0\rangle$ directions.

To the authors' knowledge this particular technique would appear to be a powerful means of studying the anisotropic distribution of stored plastic energy in brittle solids. However, further work is necessary to critically assess the application of the technique in examining the spatial distribution of plastic strain as a function of depth, load etc.

Acknowledgements

The authors are grateful to Professor R. W. K. Honeycombe for the provision of laboratory facilities and to the European Research Office of the United States Army for research support. O.O.A. also acknowledges a scholarship from the Federal Government of Nigeria.

References

1. C. A. BROOKES, J. B. O'NEILL and B. A. W. REDFERN, *Proc. Roy. Soc. London* **A322** (1971) 73.
2. J. B. O'NEILL, B. A. W. REDFERN and C. A. BROOKES, *J. Mater. Sci.* 8 (1973) 47.
3. D. J. ROWCLIFFE and G. E. HOLLOX, *ibid* 6 (1971) 1261.
4. O. O. ADEWOYE, Dissertation for the Certificate of Post-Graduate Study in Natural Sciences (Metallurgy) University of Cambridge, June 1974.
5. G. MORGAN and M. H. LEWIS, *J. Mater. Sci.* 9 (1974) 349.
6. O. O. ADEWOYE, G. R. SAWYER, T. F. PAGE and J. W. EDINGTON, (publication in preparation)
7. B. MOXLEY, Ph.D. Thesis, University of Exeter, 1974.
8. P. M. SARGENT, unpublished work, 1975.
9. O. O. ADEWOYE, G. R. SAWYER, J. W. EDINGTON and T. F. PAGE, U.S. Army (E.R.O.) Annual Technical Report, October 1974 (Contract – no. DAJA 37-74-C-1310).
10. N. W. THIBAULT and H. L. NYQUIST, *Trans. ASM* 38 (1974) 271.
11. B. W. MOTT, *Microindentation hardness testing*, (Butterworths, London, 1955).

Received 28 November
and accepted 12 December 1975

O. O. ADEWOYE
T. F. PAGE
Department of Metallurgy and Materials Science,
University of Cambridge
Pembroke Street, Cambridge, UK

The effect of environment on the creep and stress rupture behaviour of Rene 95

Previous work on Udimet 700 has indicated that an air environment could result in lower rupture life and ductility in specimens tested under conditions of creep and stress-rupture at elevated temperature [1]. Also, in cast Udimet 500, localized oxidation at grain boundaries due to the air environment has been found to play an important role in crack nucleation and propagation under conditions of elevated temperature low-cycle fatigue [2]. In addition to the above class of alloys, such effects have also been reported in steels, in which specimens tested in air were found to be prone to cavitation [3]. The present study was undertaken as a prelude to a detailed investigation of creep-fatigue interaction in Rene 95, which is a high strength nickel-base superalloy used primarily for compressor and turbine disc applications in advanced gas turbine engines. It was desired to obtain a clearer idea of the effects of air environment on the creep and stress rupture behaviour of Rene 95.

In addition to the conventional strengthening mechanisms involving precipitation of a high volume fraction of gamma-prime and, to a smaller degree, solid solution strengthening, Rene 95 derives part of its strength from the residual dislocation substructure introduced into the alloy during a thermomechanical processing treatment (TMT). This TMT is responsible for the duplex structure of Rene 95, referred to as the necklace structure, in which large warm-worked grains are surrounded by a necklace of very small recrystallized grains (Fig. 1). The necklace grains are very fine and are pinned by over-aged gamma-prime particles (Fig. 2). The warm-worked grains contain